Ce-doping effects on electronic structures of $Ba_{0.5}Sr_{0.5}TiO_3$ thin film

S Y Wang[1]**, B L Cheng**[1,3] **, Can Wang**[1]**, T W Button**[2]**, S Y Dai**[1]**,
K J Jin**[1]**, H B Lu**[1]**, Y L Zhou**[1]**, Z H Chen**[1] **and G Z Yang**[1]

[1] Beijing National Laboratory for Condensed Matter Physics, Institute of Physics, Chinese
Academy of Sciences, Beijing 100080, People's Republic of China
[2] IRC in Materials Processing, University of Birmingham, Edgbaston,
Birmingham B15 2TT, UK

E-mail: blcheng@aphy.iphy.ac.cn

Abstract

In order to clarify the basic reason why Ce doping can dramatically decrease
the leakage current in $Ba_{0.5}Sr_{0.5}TiO_3$ (BST) as reported in our previous work
(Wang *et al* 2005 *J. Phys. D: Appl. Phys.* **38** 2253), we have employed
x-ray photoelectron spectroscopy (XPS) and the optical transmittance
technique to study the electronic structure of undoped and 1.0 at% Ce-doped
BST (CeBST) films fabricated by pulsed laser deposition. XPS results show
that Ce doping has a strong influence on the valence band and core levels of
BST films, and that the Fermi level is lowered by about 0.35 eV by
Ce doping. Optical transmittance measurements demonstrate that the energy
gap is expanded with Ce doping. These Ce-doping effects can induce an
increase in the barrier height for the thermionic emission and eventually
reduce leakage current in CeBST thin films.

(Some figures in this article are in colour only in the electronic version)

1. Introduction

A resurgence of interest in barium strontium titanate (BST)
has been seen in the last decade because of its favourable
performance in tunable microwave devices, nonlinear optics
and ferroelectric random access memory (FeRAM) [1–4].
BST ($Ba_{1-x}Sr_xTiO_3$) is a continuous solid solution between
$BaTiO_3$ and $SrTiO_3$ over the whole concentration range.
The Curie temperature of BST decreases with increasing Sr
concentration [5]. As a result, the transition temperature
between the cubic and tetragonal phases, and hence the
electrical and dielectric properties of BST, can be tailored
over a broad range to meet requirements for various electronic
applications. X-ray photoelectron spectroscopy (XPS) can
provide insight into the energy distribution of occupied
electronic states in a solid material. The pioneering theoretical
work on the band-structure of $SrTiO_3$ was carried out by
Khan and Leyendecker [6], followed by Pertosa and Michel-
Calendini [7] and Soules *et al* [8]. Pertosa and Michael-
Calendini [7] studied the band structures and the density of

state (DOS) of bulk $BaTiO_3$ using the tight-binding method and
compared the theoretical results with experimental valence-
band spectra. Their theoretical results were in agreement
with XPS measurements, especially when the inner orbitals
of Ba and Ti cations had been taken into account. Reihl
et al [9] demonstrated that the total experimental DOS agreed
with the calculated results of Pertosa when the band-gap
energy was readjusted for the n-type Nb-doped $SrTiO_3$ single
crystal. Hudson *et al* [10] reported the valence and core-
level photoemission measurements from the vacuum-fractured
single-crystal $BaTiO_3$. They observed negligible band bending
on the vacuum-fractured surface of $BaTiO_3$. Furthermore,
doping in BST can strongly influence the electronic structure.
Higuchi *et al* [11] studied the electronic structure of the p-type
acceptor Sc-doped $SrTiO_3$ single crystal. They found that the
Fermi level in the p type $SrTiO_3$ crystal is lower by about 0.7 eV
than that in the n type material.

As thin films can offer advantages of light weight,
compactness, lower energy consumption in operation and
compatibility with semiconductor processing technology, BST
films have been investigated with many techniques. In the
search for alternative gate oxides to SiO_2, $SrTiO_3$ films with

---

[3] Author to whom any correspondence should be addressed.

2 nm thickness were grown on n- and p-type Si substrates [12]. Recently, Amy *et al* [13, 14] showed that surface treatment strongly affects the position of the valence-band maximum and the oxide core levels, and that the valence band offset is changed by surface treatment for $SrTiO_3$ and $BaTiO_3$ thin films with thicknesses smaller than 10 nm. As for the application in tunable microwave devices, BST films are usually deposited onto MgO substrates with thicknesses in the range of hundreds of nanometres. Therefore, the dielectric and electrical properties and the electronic structures of valence and core-level are different from the BST films deposited on Si substrate used as high-*k* dielectric materials. In our recent investigations, we found that the dielectric and electrical properties of BST thin films grown by PLD are strongly influenced by the composition and dopant in BST thin films [15–17]. For example, acceptor Co^{3+} and Ce^{3+} doping induced a decrease in the leakage current in $Ba_{0.5}Sr_{0.5}TiO_3$ films [16, 17]. It is well known that the electronic structures of materials strongly influence the dielectric, ferroelectric and electrical properties. Therefore, in this paper, we study the valence band, core levels and energy gap of Ce-doped $Ba_{0.5}Sr_{0.5}TiO_3$ (CeBST) thin films compared with undoped BST thin films. A possible correlation between transport properties and electronic structure is also discussed.

2. Experimental procedure

Undoped and CeBST thin films were grown by the PLD technique from ceramic targets prepared by conventional solid-state reaction. The detailed deposition procedure has been described in [16]. The thickness of the BST films was measured to be about 200 nm by a surface profile measuring system (DEKTAK III, USA). The crystalline structures of the BST films were analysed by x-ray diffraction (XRD) employing CuKα radiation (40 kV, 50 mA). The Rietveld powder diffraction profile-fitting technique was used to refine the crystal structure and to calculate the lattice parameter of BST targets using DBW-9411 software. XPS data were obtained by an ESCALab220i-XL electron spectrometer from VG Scientific using 300 W AlKα (1486.6 eV) radiation. The background pressure was about 3×10^{-7} Pa. The binding energies were referenced to the C 1s line at 284.6 eV from adventitious carbon. The optical transmittance of BST films was measured using an automated scanning monochromator (Varian, Cary 2390 spectrophotometer). All the measurements were performed at room temperature.

3. Results and discussion

The BST and the CeBST thin films possess a perovskite structure, as shown in figure 1, and there is a preferred orientation along the (00l) direction due to the MgO (001) substrate. The lattice parameter of undoped BST film is 3.98 Å, which is smaller than that of the CeBST film, 4.02 Å estimated from the (002) peak in the XRD spectra. These results demonstrate that Ce ions with larger radii induce the expansion of the lattice of BST thin films [17].

The XPS spectrum of a BST film in the binding energy range of 0–1200 eV is shown in figure 2. The peaks have been assigned, as indicated in the figure, and it can be seen that
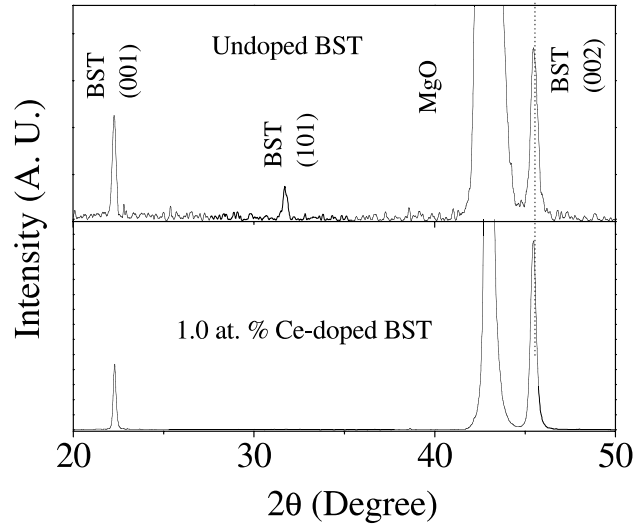

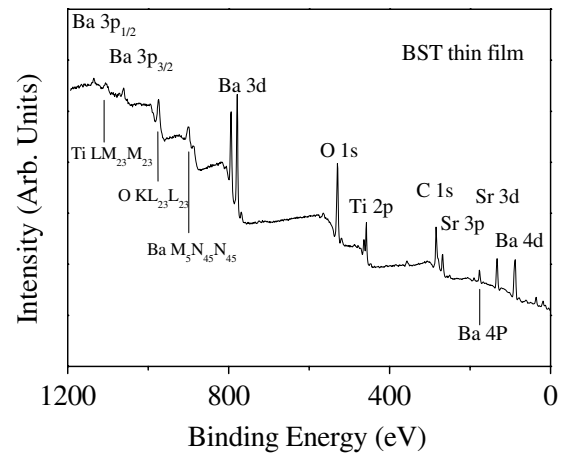**Figure 1.** X-ray diffraction spectrum of undoped and CeBST thin films on MgO substrates.

Figure 2. XPS spectrum of BST film in the binding energy range of 0–1200 eV.

Ba, Sr, Ti, O and C exist near the surface; no other impurity elements are detected in the spectrum up to 1200 eV except carbon, probably due to contamination.

The Ba 3d, Sr 3d, Ti 2p and O 1s core levels in undoped (solid symbols) and CeBST (empty symbols) thin films are shown in figures 3(*a*)–(*d*), respectively. The binding energy of Ba 3d core levels in the undoped BST thin film is 778.50 eV, and that in the CeBST film is 778.15 eV. The Sr 3d, Ti 2p and O 1s core lines are located at 132.35 eV, 457.9 eV and 529.15 eV in the undoped BST film and at 132.0 eV, 457.55 eV and 528.8 eV in the CeBST film, respectively. The experimental results demonstrate clearly that there exists a core-level shift of 0.35 eV towards the lower binding energy in the CeBST thin film.

For Ba 3d, each of the Ba $3d_{3/2}$ and Ba $3d_{5/2}$ peaks can be fitted by two peaks separated by around 1.6 ± 0.1 eV, as shown in the inset of figure 3(*a*). The lower binding energy peaks at 778.4 and 793.7 eV denoted as Ba 1 are attributed to Ba atoms in the BST perovskite lattice, and the peaks at 780.1 and 795.2 eV denoted as Ba 2 are assigned to a relaxed BST phase due to oxygen vacancies and residual defects [2]. As for
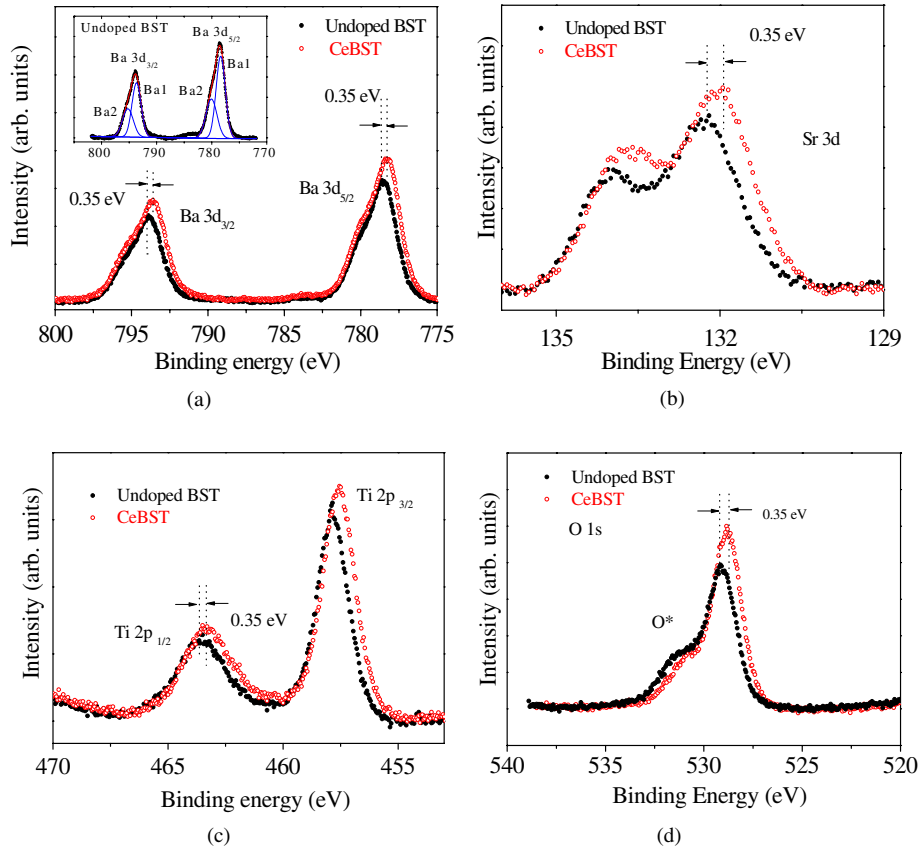
Figure 3. XPS spectra of the Ba 3d (*a*), Sr 3d (*b*), Ti 2p (*c*) and O 1s (*d*) core levels of undoped and CeBST films. The inset in (*a*) is the fitted XPS spectrum of the Ba 3d region for the undoped BST thin film.

oxygen, it is observed that the O 1s line is composed of two peaks, as shown in figure 3(*d*). One of these peaks (O_{ox}) is located at a lower binding energy of 529.0 eV, but the other peak (O*) is shifted about 2.5 eV towards the higher binding energy. These two peaks may correspond to two types of oxygen atoms. The former can be attributed to the main peak of oxygen atoms in the perovskite BST lattice, while the latter can be ascribed to hydroxyl groups on the film surface [18].

The shallow core-level photoelectron spectrum from 0 to 28 eV with inelastic background fitting of the BST film is shown figure 4. The inset in the figure is the valence-band photoelectron spectrum of the BST film. Labels A, B and C are used to denote the mainly O 2p-derived emission features as in the earlier ultraviolet and x-ray photoemission works [9, 10]. Features D and E, ranging from 10 to 15 eV in the binding energy, are composed of the Ba $5p_{1/2}$-$5p_{3/2}$ spin–orbit splitting of the BST film, as observed by Pertosa and Michel-Calendine [7]. Feature F centred at around 18 eV is composed of Sr 4p, and the O 2s level gives rise to a broad shoulder (G) on the higher binding-energy side of feature F. The energy at the top of the valence band is determined from the intercept of a linear fit to the right shoulder of feature A with a zero line. Hence, as shown in inset of figure 4, the top of the valence band is located at about 0.6 eV lower than the Fermi level. This implies that the Fermi level is not located at the centre of the energy gap but very close to the valence band in the energy gap. The band-gap value of the BST film determined from the optical transmittance spectrum
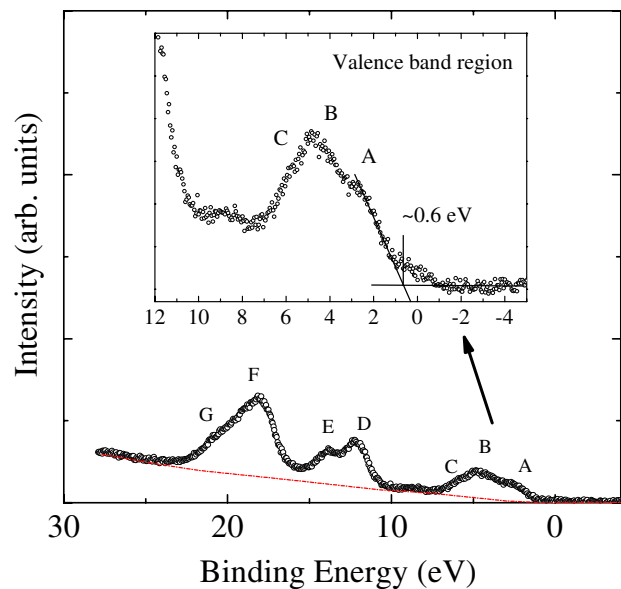

Figure 4. Shallow core-level and valence band photoelectron spectrum for the undoped BST film. The inset shows the valence band spectrum.

is estimated as 3.65 eV, as shown in the following part. Such a phenomenon can be ascribed to the band bending effect at the BST film surface [10, 19].

The valence bands of the undoped BST and CeBST films in the binding energy scale from −5 to 10 eV are presented in
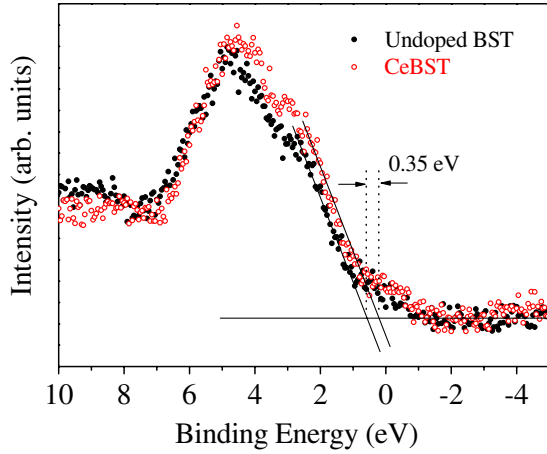
Figure 5. The comparison of the valence band spectra between the undoped and the CeBST films.
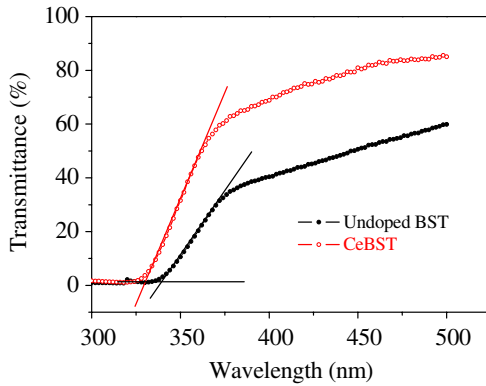

Figure 6. Optical transmission as a function of the wavelength of the undoped and CeBST thin films on MgO substrate.

figure 5. Although the profiles of the valence band for the two samples are similar, it can be clearly seen that the position of the valence-band top is shifted to a lower binding energy by about 0.35 eV in the CeBST thin film. This result seems to be consistent with the energy shifts in Ti, Ba, Sr and O core lines, which means that the Fermi level becomes lower in the CeBST films. In our previous work [16], XPS results of Ce 3d showed that Ce was trivalent as an acceptor in the CeBST thin film, which results in a p-type film in CeBST. Therefore, the core levels and the Fermi level will shift in the CeBST thin films. Higuchi et al. [11] observed the similar effect in a Sc-doped SrTiO$_3$ single crystal compared with a Nb-doped SrTiO$_3$ single crystal, that is, the Ti lines and valence-band top undergo a core-level shift to a lower binding energy.

The CeBST films are highly transparent with a transmittance of more than 60%, which is higher than that of the undoped BST film in most of the visible spectrum, as shown in the optical transmittance spectra in figure 6. The absorption edge in an optical transmittance spectrum of the CeBST thin films at 300–400 nm is attributed to the electron transition from the valence band to the conduction band [20]. The absorption edge of the films is 339.5 nm ($h\nu = 3.65$ eV) and 330.9 nm ($h\nu = 3.75$ eV) for undoped and CeBST thin films, respectively in figure 6. Thus, the energy gap of CeBST films increases with Ce concentration. Guo *et al* [20] observed

a similar effect in In-doped SrTiO$_3$ films, that is to say, the In^{3+} resulted in the expansion of the width of the band gap. We ascribe the expansion of the energy gap of BST films to the change in the lattice parameter due to the Ce dopant.

According Harrison's model [21, 22], the energy gap (E_g) can be expressed by

$$E_g = \varepsilon_d - \varepsilon_p - 2\sqrt{2}(V\mathrm{pp}\sigma + V\mathrm{pp}\pi), \qquad (1)$$

where the ε_d is the energy of the Ti 3d orbital, ε_p is the energy of the O 2p orbital, $V\mathrm{pp}\sigma$ is the σ bonding energy of the neighbouring O 2p, and $V\mathrm{pp}\pi$ is the π bonding energy of the neighbouring O 2p orbital. $V\mathrm{pp}\sigma$ and $V\mathrm{pp}\pi$ change with the interatomic distance (d), as follows:

$$V\mathrm{pp}\sigma + V\mathrm{pp}\pi = (\eta_{pp\sigma} + \eta_{pp\pi})\left(\frac{h^2}{m}\right)d^{-n}, \qquad n > 0, \tag{2}$$

where $\eta_{pp\sigma}$, $\eta_{pp\pi}$ and n are dimensionless coefficients, h is Planck's constant, m is the electron mass and d is the distance between the neighbouring oxygen atoms. In CeBST films, as mentioned earlier, the Ce doping increases the lattice constant of film, which can decrease the value of ($V\mathrm{pp}\sigma + V\mathrm{pp}\pi$), as illustrated in equation (2), resulting in an increase in the energy gap E_g. Thus, the expansion of the energy gap may due to an increase in the lattice constant induced by doping with larger Ce atoms.

In the application of BST thin films, high electric insulation with low leakage current is one of the crucial factors. To achieve high insulation, dopants, such as Mn$_2$O$_3$ [23], Ce$_2$O$_3$ [16], Co$_2$O$_3$ [17], etc have been adopted with good results. Various mechanisms have been proposed to explain the change in the leakage current. It is proposed that the depletion layer width or the barrier height is inversely proportional to the net donor concentration in the BST film. When doped with acceptors, both the depletion layer width and the barrier height become larger, making it more difficult for the electrons to pass through the potential barrier, which results in a decrease in the tunnelling and thermal emission currents. Furthermore, Copel *et al* [23] have investigated the effects of Mn impurities in BST thin films using XPS, and they found that Mn acts as an electron acceptor, compensating for the carrier density in undoped BST. As discussed earlier, in CeBST thin films, the Fermi level is shifted closer to the valence band and the energy gap is expanded. These effects can increase the distance from the Fermi level to the conduction band in the CeBST thin films, contributing to the increase in the barrier height for thermionic emission of electrons from the electrode into the CeBST. Therefore, the CeBST will exhibit a higher barrier for thermionic emission of electrons, which can give rise to a reduced thermionic emission and a decreased leakage current. We have observed in a Pt/BST/Nb-SrTiO$_3$ capacitor that Ce doping decreases the leakage current [16].

4. Conclusions

The XPS and the optical transmittance spectrum investigation on undoped BST and CeBST films demonstrated a strong influence of Ce doping on the electronic structures. Ce doping induced a shift of the core level peaks and the valence-band

top to a lower binding energy; it resulted in a shift of the Fermi level of BST film towards the valence band; it also induced an expansion of the energy gap width in the BST thin film. These variations of electronic structure are responsible for the reduction of leakage current in the CeBST thin film.

Acknowledgments

References

[1] Sirenko A A, Bernhard C, Golnik A, Clark A M, Hao J, Si W and Xi X X 2000 *Nature* **404** 373
[2] Cracium V and Singh R K 2000 *Appl. Phys. Lett.* **76** 1932
[3] Ramesh R, Inam A, Chan W K, Wilkens B, Myers K, Remschnig K, Hart D L and Tarascon J M 1991 *Science* **252** 944
[4] Nagarajan V *et al* 2004 *Appl. Phys. Lett.* **84** 5225
[5] Gim Y, Hudson T, Fan Y, Kwon C, Findikoglu A T, Gibbons B J, Park B H and Jia Q X 2000 *Appl. Phys. Lett.* **77** 1200
[6] Khan A H and Leyendecker A J 1964 *Phys. Rev.* **135** A1321
[7] Pertosa P and Michel-Calendini F M 1978 *Phys. Rev.* B **17** 2011
[8] Soules T F, Kelly E J, Vaught D M and Richardson J W 1972 *Phys. Rev.* B **6** 1519
[9] Reihl B, Bednorz J G, Muler K A, Jugnet Y, Landgren G and Morar J F 1984 *Phys. Rev.* B **30** 803
[10] Hudson L T, Kurtz R L, Robey S W, Temple D and Stockbauer R L 1993 *Phys. Rev.* B **47** 1174
[11] Higuchi T, Tsukamoto T, Sata N, Ishigame M, Tezuka Y and Shin S 1998 *Phys. Rev.* B **57** 6978
[12] Chambers S A, Liang Y, Yu Z, Droopad R, Ramdani J and Eisenbeiser K 2000 *Appl. Phys. Lett.* **77** 1662
[13] Amy F, Wan A S, Kahn A, Walker F J and Mckee R A 2004 *J. Appl. Phys.* **96** 1635
[14] Amy F, Wan A S, Kahn A, Walker F J and Mckee R A 2004 *J. Appl. Phys.* **96** 1601
[15] Wang S Y, Cheng B L, Wang C, Peng W, Lu H B, Zhou Y L, Chen Z H and Yang G Z 2005 *Key Eng. Mater.* **280–283** 81
[16] Wang S Y, Cheng B L, Wang C, Dai S Y, Jin K J, Lu H B, Zhou Y L, Chen Z H and Yang G Z 2005 *J. Phys. D: Appl. Phys.* **38** 2253
[17] Wang S Y, Cheng B L, Wang C, Dai S Y, Lu H B, Zhou Y L, Chen Z H and Yang G Z 2004 *Appl. Phys. Lett.* **84** 4116
[18] Chambers S A, Liang Y, Yu Z, Droopad R and Ramdani J 2001 *J. Vac. Sci. Technol.* A **19** 934
[19] Scott J F 2000 *Ferroelectric Memories* (Heidelberg: Springer)
[20] Guo H Z, Liu L F, Fei Y Y, Xiang W F, Lu H B, Dai S Y, Zhou Y L and Chen Z H 2003 *J. Appl. Phys.* **94** 4558
[21] Kohiki S, Arai M, Yoshikawa H, Fukushima S, Oku M and Waseda Y 2000 *Phys. Rev.* B **62** 7964
[22] Zhu J S, Lu X M, Jiang W, Tian W, Zhu M, Zhang M S, Chen X B, Liu X and Wang Y N 1996 *J. Appl. Phys.* **81** 1392
[23] Copel M, Baniecki J D, Duncombe P R, Kotecki D, Laibowitz R, Neumayer D A and Shaw T M 1999 *Appl. Phys. Lett.* **73** 1832